Damage and Failure Model Characterization for High Strength AA6000 Automotive Aluminium Alloys

Sebastijan Jurendic[1], Richard Burrows[2], David Anderson[2]
[1]Novelis Deutschland GmbH, R&D Centre Göttingen, Germany
[2]Novelis inc., Novelis Global Research and Technology Center, Kennesaw, USA

Abstract

In this work we compare two different approaches for characterizing the GISSMO damage and failure model for high strength AA6000 series aluminium alloys using LS-DYNA®. The aim is to determine a consistent and reliable procedure for determining failure related mechanical properties of the material for use in automotive crash applications. The two approaches considered here are: a) an inverse numerical technique using LS-OPT® to solve an optimization problem and b) direct measurement of material data using specific mechanical tests and digital image correlation. The material data determined by both approaches is compared and evaluated for accuracy using the GISSMO test geometries and a comparison between shell elements and solid elements is given.

Introduction

This work focuses on characterizing and modelling the mechanical behaviour of a AA6000 series high strength heat treatable aluminium alloy, both in terms of plasticity as well as material damage and failure. The material considered here is a representative AA6000 series aluminium alloy sheet in the peak aged and paint baked state of temper, as might be used for body-in-white construction in the automotive industry [1]. The goal is to determine a practical and reliable procedure of determining the material properties necessary for application of the GISSMO damage and failure model. These consist of the work hardening behaviour of the material during plastic deformation and the fracture locus in the triaxiality – strain to failure space.

Two approaches for characterizing the material properties are evaluated in this work: firstly, the inverse numerical approach, solving an optimization problem to achieve a best fit over several load cases [2] and secondly, a physically based approach, consisting of measuring the hardening behaviour using an in-plane torsion test [3] and direct measurement of the failure locus using different tests and digital image correlation (DIC) [4]. Results from both methods are compared and evaluated for accuracy. Four GISSMO test specimen geometries, as defined in [2], are used to validate the material models response.

Material properties characterization

Inverse numerical method

The inverse method applied here is extensively described in previous works [2, 5, 6]. In summary, this method involves mechanical testing of several material coupon designed to cover a broad spectrum of triaxiality states, from shear to biaxial tension. The mechanical tests are then re-created in a numerical simulation in order to iteratively solve the optimization problem of minimizing the difference between the measured and simulated material response. This approach was utilized to determine both the work hardening properties of the material as well as the damage and failure parameters.

The work presented here was performed by an external collaboration partner. Five plus one geometries were used to determine the material response. The five geometries, shown on Figure 1, are used for the solving the inverse problem. An additional geometry based on the standard ISO tensile test with a gauge length of 80 mm is used to determine the regularization curve for the damage and failure loci.

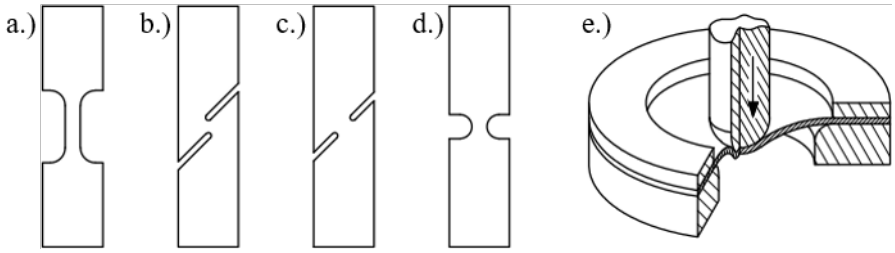

Figure 1: Specimen geometries used in the inverse numerical method: a.) small scale tensile test, b.) plane strain tests, c.) 0° shear test, d.) 45° shear test and e.) biaxial indentation test.

Since the inverse numerical method is directly linked to the simulation parameters implemented in the numerical models of the physical tests, three cases employing different material model set-ups were considered:

- Case 1: Fully isotropic Von Misses material model,
- Case 2: Barlat 89 yield locus, forced in-plane isotropic by using a single average R-value and using one work hardening curve and
- Case 3: Barlat 89 yield locus with three R values and three work hardening curves in the longitudinal, diagonal and transverse direction.

In all cases, fully integrated quadrilateral shell elements with a representative edge length of 0.5 mm were used.

Direct measurement method

The direct measurement approach consists of two parts: determining the work hardening response and determining the fracture locus. These are two distinct tasks that are completely independent from each other. The activities were performed by two unaffiliated external collaboration partners.

The work hardening response was determined using the in-plane torsion test [3] schematically shown on Figure 2. This test shows good results in determining the mechanical properties of materials to very high strains using shear deformation. There is no inherent geometrical mode of deformation which would cause localized instability or stress localization in this test, meaning that the material is loaded uniformly to failure. The stress is determined using analytical relations from the measured torque on the specimen and the strain is determined by using DIC to measure the deformation gradient on the surface of the specimen.

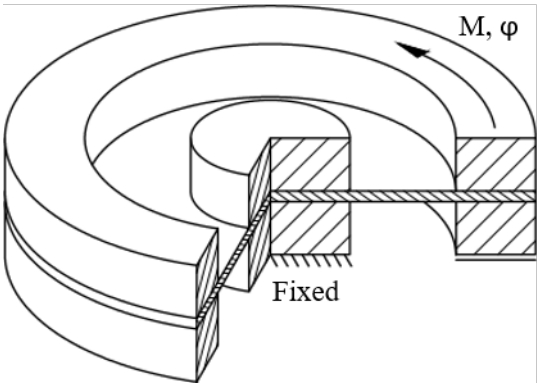

Figure 2: Schematic representation of the in-plane torsion test.

A grooved specimen geometry [3] was used in this investigation, prepared by milling out a circumferential groove on both sides of the specimen. This serves to concentrate the shear deformation in the groove, away from the clamping fixture, thus avoiding the stress concentration and allowing higher strains to be achieved.

To determine the failure locus of the material, four tests with a linear stress path to failure were implemented [4]: a.) simple shear, triaxiality = 0, b.) hole expansion, triaxiality = 0.33, c.) V-bend test, triaxiality = 0.6 and d.) hemispherical punch indentation, triaxiality = 0.667, as shown on Figure 3. DIC strain measurement was used to determine the strains to failure for each specimen.

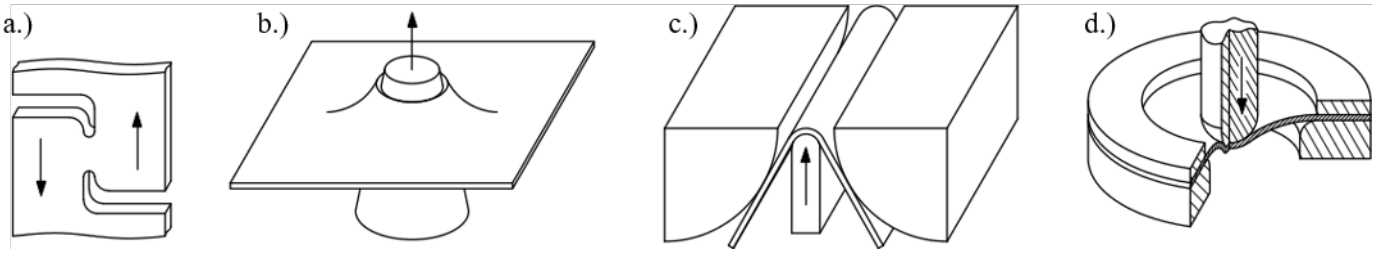

Figure 3: Schematic representation of the fracture locus determination tests: a.) simple shear, b.) hole expansion, c.) V-bend test and d.) hemispherical punch indentation.

The hemispherical punch indentation test is carried out using two deferent punch diameters, 25.4 mm and 50.8 mm to create two different states of biaxial bending. In addition to the tests listed above, a uniaxial tensile test is also carried out to establish an alternative failure point in uniaxial tension.

Identified material properties

Inverse numerical method

The material properties identified by the inverse numerical method are shown on Figure 4. True stress – true plastic strain work hardening curves and the effective plastic strain to failure – triaxiality curves were determined for the three material model cases defied above.

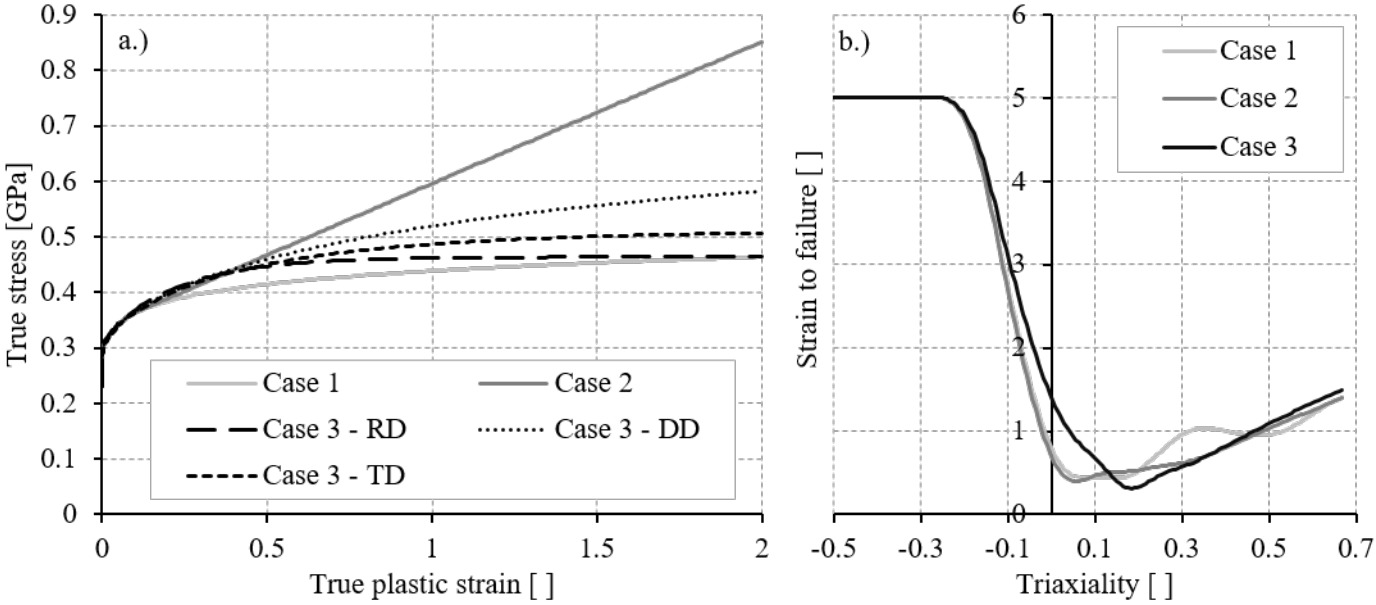

Figure 4: Inversely identified material properties: a.) work hardening curves and b.) failure loci for the three material model variants.

The results clearly demonstrate the strongly dependency of the inverse numerical method on the properties of the implemented numerical models. Large variations in the identified material properties can be seen between the three cases, both in the work hardening properties as well as the damage and failure curves. The identified work hardening curves show large variation in shape and stress levels across the three variants which in itself is not consistent with trying to identify an intrinsic property of the material. Furthermore, none of the identified work hardening curves are consistent with the actual hardening behaviour that was determined using measurements. Finally, in the third case, where separate hardening curves are defined for the relevant in-plane directions, the three directions show significant differences in their work hardening behaviour, which is not physically representative for an aluminium material.

Direct measurement method

In the case of the direct measurement approach, the equivalent true stress – true strain curve measured with the in-plane torsion test is shown below on Figure 5. Reliable data to very high strains could be attained using this method.

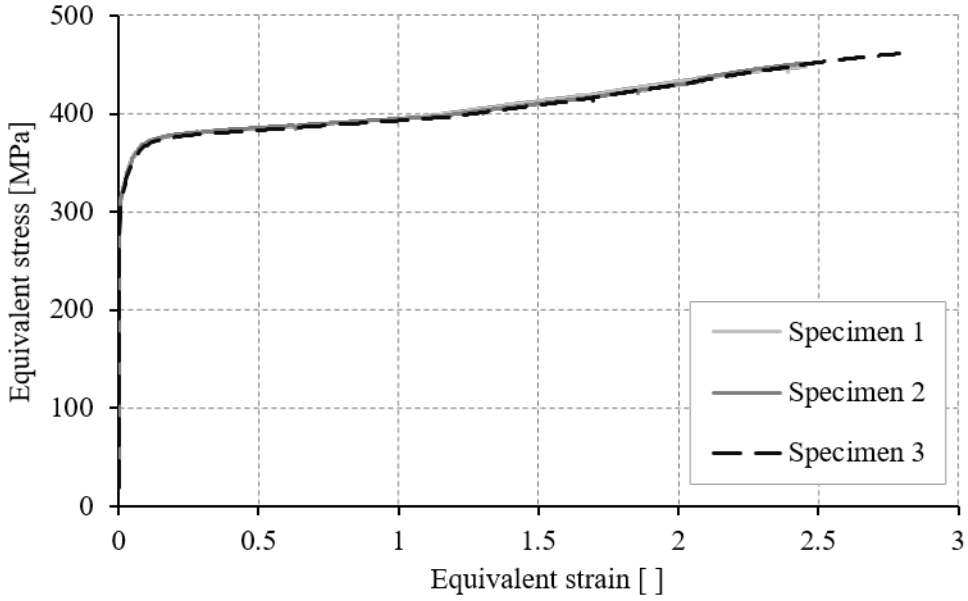

Figure 5: Equivalent stress – equivalent strain curves measured by the in-plane torsion test.

The measured data extends to well over a strain of 2, which all but eliminates the need for extrapolation when creating the work hardening curves for use in finite element simulations. The hardening behaviour of the material at high strains can be clearly established from this data, without the need for an inverse numerical approach. For this particular aluminium alloy, after the initial work hardening phase, a region of linear hardening sets in. A slight inflection of the linear trend occurs strains of approximately 1.2, the origins of which are not fully understood at this point. While it might be an intrinsic property of the material, the possibility that it is an artefact of the testing method must be considered. The initial onset of the inflection in this case coincides with the first re-application of the painted speckle pattern for the DIC system. Due to the high strains achieved in the test, the distortion of the speckle pattern becomes too great for the DIC system to follow. To alleviate this effect, the test is interrupted and the sample is re-painted. In the current work the samples were re-painted 3 or 4 times, however, the inflection occurred only around the first interruption of the test. Further investigation is needed on this topic.

The results of experimentally determining the fracture locus are shown on Figure 6. Two different failure loci can be interpreted from the acquired data, one which includes the V-bend test and the small diameter hemispherical punch and the other including the uniaxial tensile test and the larger diameter punch. Higher

failure strains are achieved in the first case and the shape of the failure locus is somewhat different. In the latter case the classical "W" shaped yield locus is identified.

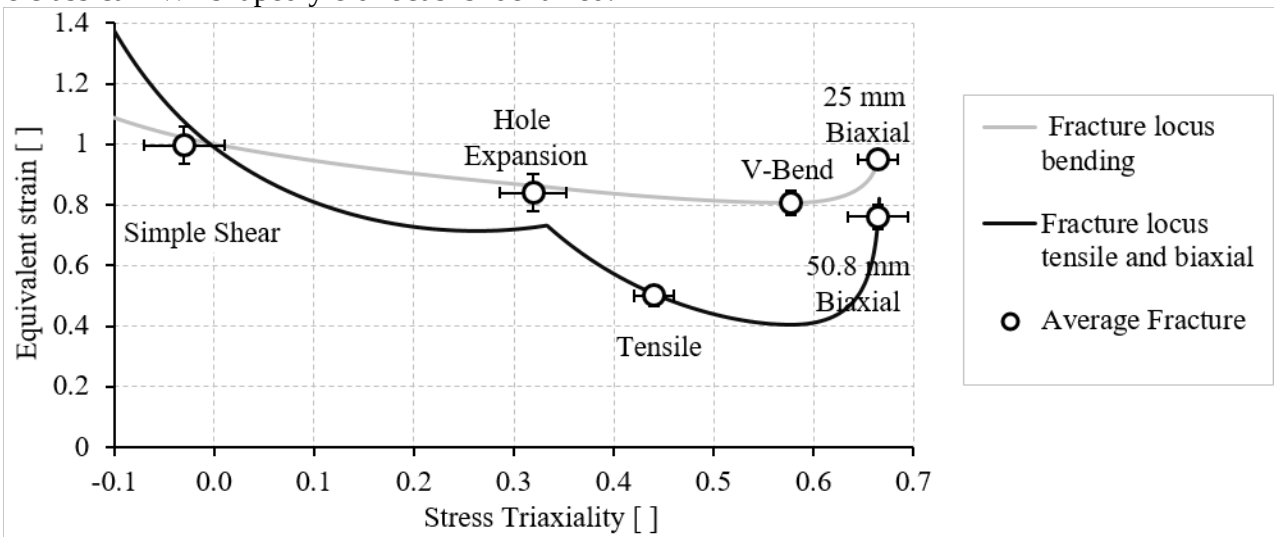

Figure 6: Failure loci determined by direct measurement of material fracture.

The interpretation of the data is not yet fully understood, however, one possible explanation is that the bending, be it in plane strain or biaxial, supresses the onset of localized deformation through thickness and results in higher strain being achieved before material fracture occurs. Also of note is the fact that the torsion test also achieves significantly higher strains the shear deformation than the simple shear test.

Validation

To validate the performance of the identified material properties, models of four GISSMO test coupons were created (Figure 7) and simulated using the various data sets, the resulting force – extension responses were then compared to the measured data. Firstly, a detailed solid element model was created to establish a baseline model response using the physically measured material data. Secondly, models using shell elements were created to directly compare the behaviour of the different data sets with each other in a manner more representative of industrial applications.

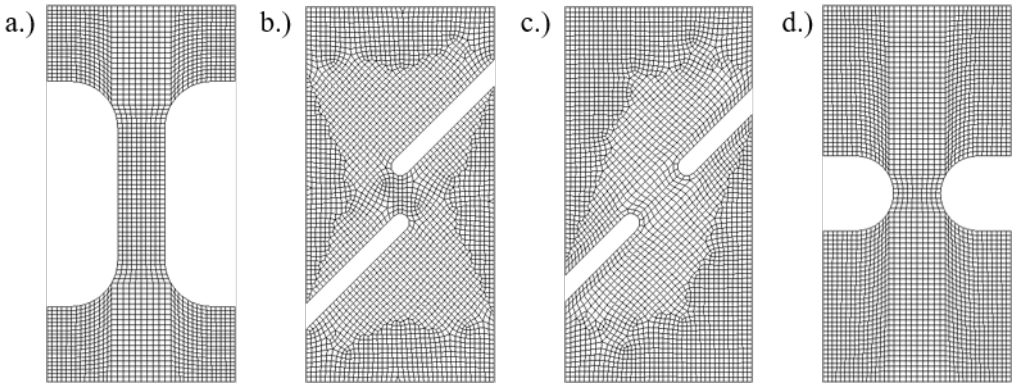

Figure 7: Finite element models of the GISSMO specimens: a.) small scale tensile test, b.) 0° shear test, c.) 45° shear test and d.) plane-strain test.

Solid element models

The solid element model was used in conjunction with the physical measure material data, the identified "W" shaped fracture locus was implemented. The coupons were modelled using fully integrated hexahedron

solid elements, with a representative element size of approximately 0.5 mm. No mass scaling or symmetry conditions were used, however, the solution was time scaled to a total simulated deformation time of 0.1 s, which was found to provide an acceptable compromise between accuracy and computation time. The double precision version of the LS-DYNA executable was used in all computations. The resulting load – extension responses are shown on Figure 8 below, along with the measured data from the physical tests.

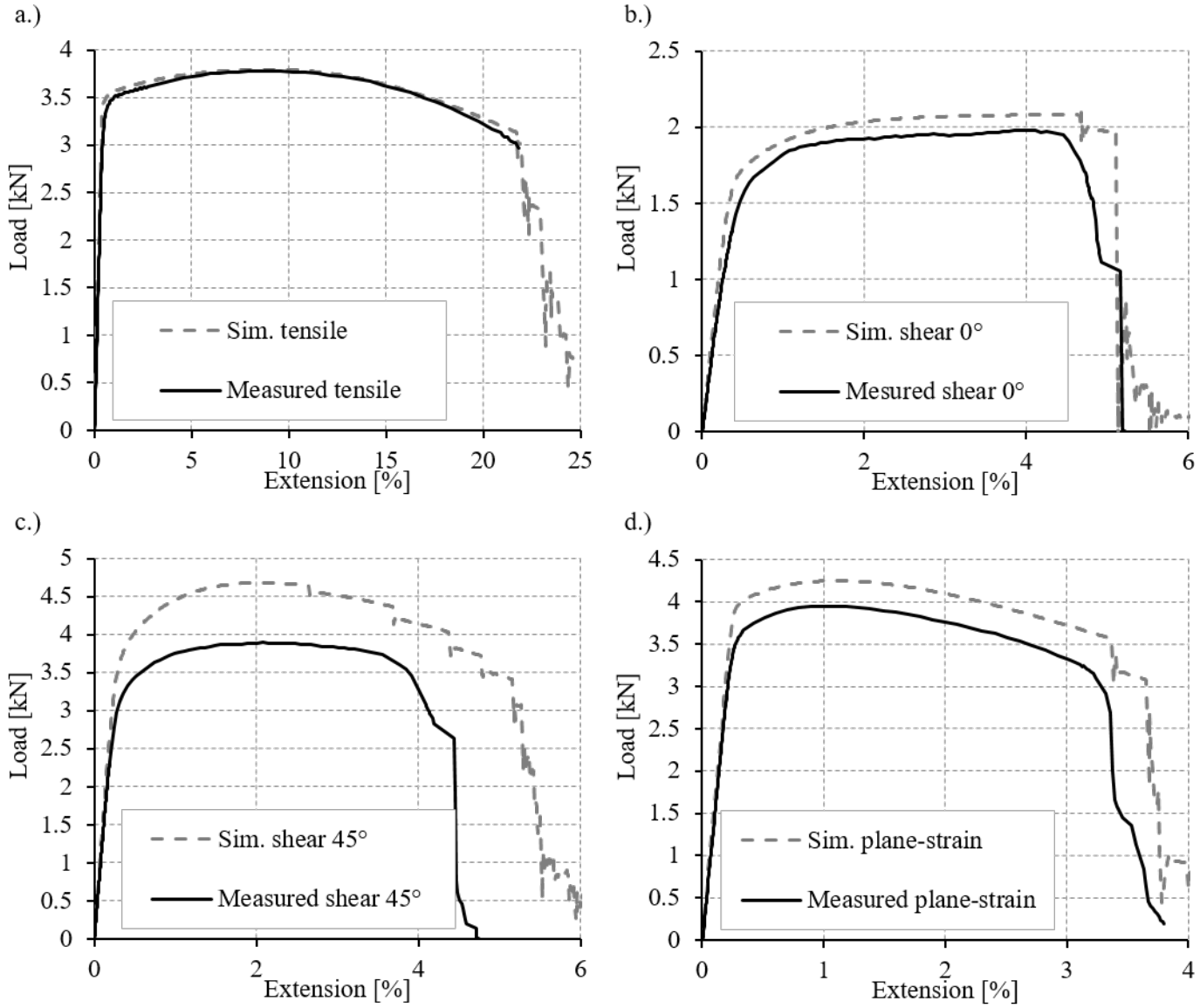

Figure 8: Load – extension plots, solid element models, simulation vs. test for four specimen geometries: a.) small scale tensile test, b.) 0° shear test, c.) 45° shear test and d.) plane-strain test.

The solid element models show generally good agreement with the experimentally measured data. While the absolute force levels deviate somewhat from the measured values, the shapes of the curves are fairly consistent for all the tests, with post-localization behaviour being captured relatively accurately. The overall stress levels could potentially be better reproduced by applying an appropriate anisotropic yield locus. The 45° shear specimen shows the poorest agreement, with a force over-prediction of approximately 15%. The total extension at failure is reproduced with similar accuracy as the force – extension behaviour, the 45° shear specimen showing the largest discrepancy in this case as well. This demonstrates that, at this level of discretization (i.e. 0.5 mm solid elements), the "W" shaped fracture locus represents the material behaviour relatively well.

Shell element models

In the second stage, the identified material data sets were used in conjunction with shell element models of the same GISSMO test geometries. Fully integrated quadrilateral shell elements were used, with a representative edge length of 0.5 mm. Other simulation parameters were kept same as with the solid element models. In the Figure 9 below, the resulting load – extension responses are shown. The simulation data is labelled as follows: Direct: material data identified through direct measurement, Inv. 1: inversely identified material data case 1, Inv. 2: inversely identified material data case 2, and Inv. 3: inversely identified material data case 3.

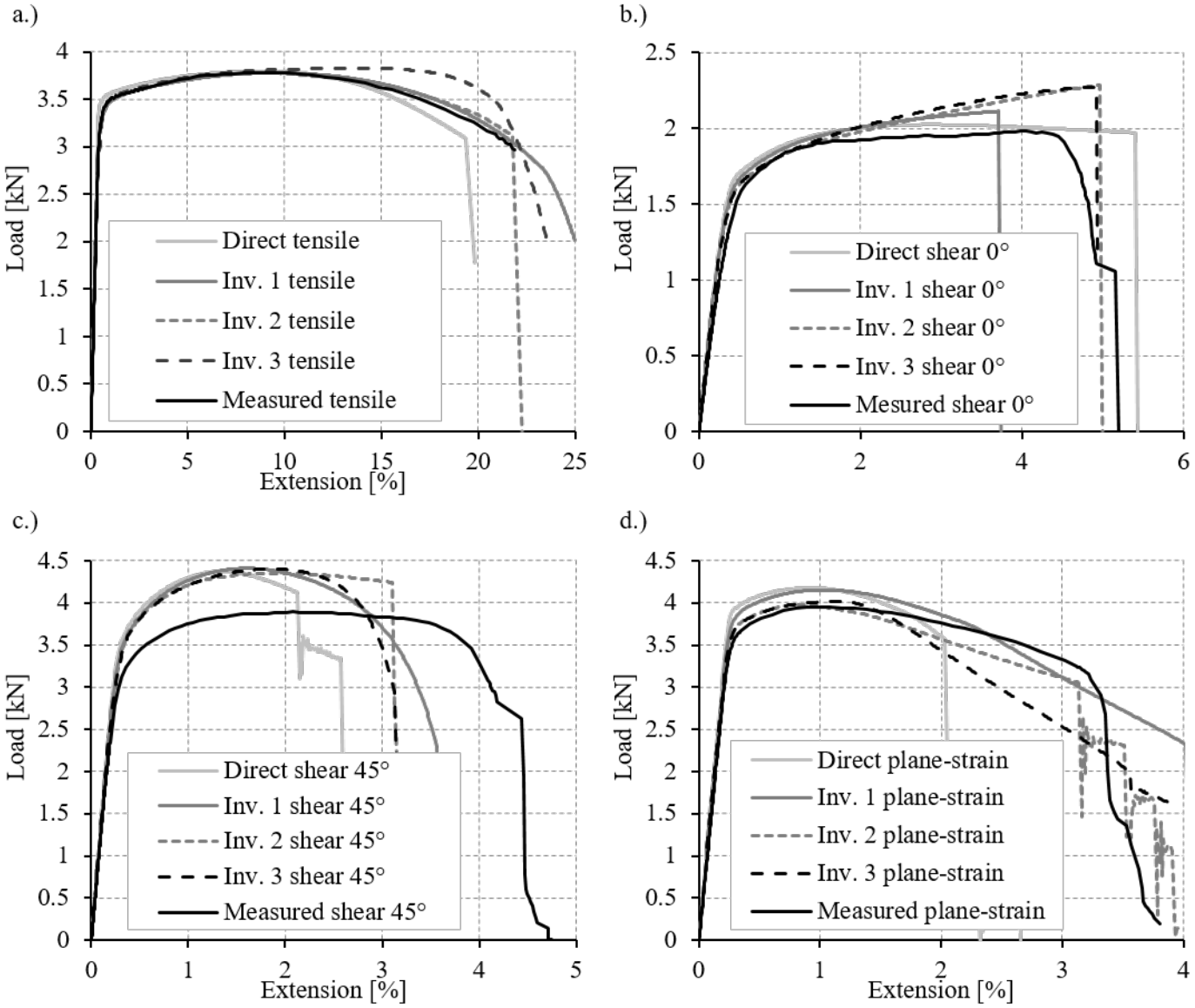

Figure 9: Load – extension plots, shell element models with different material properties, simulation vs. test for four specimen geometries: a.) small scale tensile test, b.) 0° shear test, c.) 45° shear test and d.) plane-strain test.

The different material data sets result in a large scatter of simulated material responses. The performance of the shell element models in comparison to the solid element models is poor, none of the proposed data stets produce satisfactory agreement between the simulation and the test results for all geometries. The physically derived material data in particular shows significant under-prediction of both the loads as well as extensions at

failure for all geometries except the 0° shear. This might be connected with the fact that the work hardening behaviour was identified using a shear test. Inversely identified material data sets show varying degrees of agreement across the sample geometries, with no identifiable pattern. Best agreement can be attributed to the Case 2 data set, which shows nearly perfect fit in the tensile test and best fits in the 45° shear and plane-strain tests, but significant over-prediction in the 0° shear test.

Conclusions

Two different approaches to material data identification for numerical modelling with material failure are presented in this work, both with their respective advantages and disadvantages. The inverse numerical approach should provide a good fit between the measured and simulated material response per definition, however, its application in this work showed somewhat limited success. Reasonably good agreement could be achieved for most, but not all, stress states only with one of the three material model implementations used. This may be attributed to the intrinsic limitations of shell element formulations in modelling material instability, since the solid element model could predict the materials response significantly better. What is more, as has been clearly demonstrated here, the results of the inverse method are inseparable from the properties of the models used in the identification process and cannot be interpreted as intrinsic material properties. Even though the material response could be reproduced somewhat accurately using shell elements and the inversely identified material data, the large variance between the different material models and deformation modes put into question how such a model would perform in a general simulation case.

The physically derived material properties, on the other hand, showed promising correlation in the solid element model, indicating that such data is in fact representative of the intrinsic material behaviour. However, significantly worse performance in comparison to the inversely identified data, when applied to the shell element models, further confirming the drawbacks of shell element formulations. If shell element models are used in material failure simulations, a deviation from the actual mechanical properties of the material may be necessary and indeed warranted to achieve best results. This puts a large emphasis on sufficient validation of the models before applying them to general simulation cases.

References

[1] J. Hirsch. 1997. Aluminium Alloy for Automotive Application. Material Science Forum **242** pp. 33-50

[2] J. Effelsberg, M. Feucht. 2014. Identifikation von Materialparametern mit LS-OPT – GISSMO und andere Anwendungen. Infotag LS-OPT, Stuttgart.

[3] H. Traphoener, T. Clausmeyer, A. E. Tekkaya. 2018. Material Characterization for Plane and Curved Sheets Using the In-plane Torsion Test – An Overview. Journal of Materials Processing Technology **257**, pp 278-287.

[4] C. Butcher, J. Dykemann. 2017. Great Designs in Steel. Automotive Applications Council.

[5] J. Effelsberg, A. Haufe, M. Feucht, F. Neukamm, P. Du Bios. 2012. On Parameter Identification for the GISSMO Damage Model. 11th LS-DYNA Forum, Ulm.

[6] A. Haufe A, F. Neukamm, M Feucht, P. Du Bois, T. Borvall. 2010. A Comparison of Recent Damage and Failure Models for Steel Materials in Crashworthiness Application in LS-DYNA. 11th International LS-DYNA Users Conference, Detroit.